Journal of Ayurveda and Integrative Medicine 14 (2023) 100750

Contents lists available at ScienceDirect

Journal of Ayurveda and Integrative Medicine

journal homepage: http://elsevier.com/locate/jaim

Original Research Article

Binding modes of potential anti-prion phytochemicals to PrP^C structures *in silico*

Sandesh Neupane [a, **], Jenisha Khadka [a], Sandesh Rayamajhi [a], Arti S. Pandey [b, *]

[a] Purbanchal University, Department of Biotechnology, SANN International College, Kathmandu, 44616, Nepal
[b] Department of Biochemistry, Kathmandu Medical College (Basic Sciences), Bhaktapur, 44800, Nepal

ARTICLE INFO

Article history:
Received 24 August 2020
Received in revised form
13 March 2023
Accepted 14 June 2023
Available online xxx

Keywords:
anti-Prion
Phytochemicals
Terpenes
Quinones
Sterols
Pharmacokinetics

ABSTRACT

Background: Prion diseases involve the conversion of a normal, cell-surface glycoprotein (PrP^C) into a misfolded pathogenic form (PrP^{Sc}). One possible strategy to inhibit PrP^{Sc} formation is to stabilize the native conformation of PrP^C and interfere with the conversion of PrP^C to PrP^{Sc}. Many compounds have been shown to inhibit the conversion process, however, no promising drugs have been identified to cure prion diseases.
Objective: This study aims to identify potential anti-prion compounds from plant phytochemicals by integrating traditional ethnobotanical knowledge with modern *in silico* drug design approaches.
Materials and methods: In the current study medicinal phytochemicals were docked with swapped and non-swapped crystal structures of PrP^C *in silico* to identify potential anti-prions to determine their binding modes and interactions.
Results: Eleven new phytochemicals were identified based on their binding energies and pharmacokinetic properties. The binding sites and interactions of the known and new anti-prion compounds are similar, and differences in binding modes occur in structures with very subtle differences in side chain conformations. Binding of these compounds poses steric hindrance to neighbouring molecules. Residues shown to be associated with the inhibition of PrP^C to PrP^{Sc} conversion form interactions with most of the compounds.
Conclusion: Identified compounds might act as potent inhibitors of PrP^C to PrP^{Sc} conversion. These might be attractive candidates for the development of novel anti-prion therapy although further tests *in vitro* cell cultures and *in vivo* mouse models are needed to confirm these findings.

1. Introduction

Prion diseases are fatal neurodegenerative diseases caused by the conversion of a normal, cell-surface glycoprotein (PrP^C) into a misfolded pathogenic form (PrP^{Sc}), which results in a wide array of degenerative neurological disorders [1,2]. The more stable PrP^{Sc} (also referred to as PrP^{res} for protease-resistance) denotes scrapie associated prion protein which are misfolded, beta-sheet-rich structures with low Gibbs free energy [3,4].

To date no medication has been shown to halt or even slow prion or other neurodegenerative conditions [5]. All putative anti-Transmissible Spongiform Encephalopathy (anti-TSE) drugs tested to date are prophylactic rather than therapeutic [6,7]. Many anti-prion compounds like suramin, pentosanpolysulfate, amphotericin B, cyclodextrins, phenothiazine, statin [8], doxycycline, Congo red, rapamycin, dendritic polyamines, polyphenol, diphenylpyrazolebisacridine, anti-histamine, and some anti-malarial agents including quinacrine, mefloquine, etc., have been reported to inhibit PrP^{Sc} formation or to reduce the level of PrP^C *in vitro*. Anti-PrP^C antibodies, aptamers, and intrabodies/nanobodies have shown to inhibit the prion conversion *in vitro* [9,10]. However, they were not useable because of their toxicity and inability to cross the blood–brain barrier (BBB) [11].

High throughput virtual screening and structure-based drug design are cost-effective and speed up the drug discovery process [12]. Many compounds identified through such *in silico* screening methods are under clinical trials or have been approved for therapeutic use [13–15]. Compounds like GN8 (2-pyrrolidin-1-yl-N-[4-

* Corresponding author.
** Corresponding author.
E-mails: saneaupane@gmail.com, arti.pandey69@gmail.com
Peer review under responsibility of Transdisciplinary University, Bangalore.

https://doi.org/10.1016/j.jaim.2023.100750

[4-(2-pyrrolidin-1-yl-acetylamino)-benzyl]-phenyl]-acetamide) [16], GJP49 (8-Methyl-7-{[2-(1-piperidinyl)ethyl]sulfanyl}-2,3-dihydro [1,4]dioxino [2,3-g]quinoline) [17], ellagic acid, curcumin pentagalloylglucose [18], polydatin [19], and LD7 (Phenethyl Piperidines) [20] have been shown to stabilize PrP^{C} and prolong the survival of the mice infected with prions. Recently, flavonoids baicalein and baicalin (baicalein 7-O-glucuronide), the active compounds from the North American traditional medicinal herb *Scutellaria lateriflora*, were found to reduce PrP^{Sc} accumulation in scrapie-infected cell cultures and cell-free conversion assays [21].

The science of ethnobotany has contributed to natural product research for the development of drug molecules or ethnobotanical leads. A wide range of Central Nervous System (CNS) active medicinal plants with resins and volatile oils are used in different cultures to treat headaches, improve mood, alter perceptions, and improve CNS health [22,23]. In this study, we have integrated traditional ethnobotanical knowledge with *in silico* Computer Aided Drug Designing for the identification of potential plant derivative compounds that might inhibit the pathogenic conversion of PrP^{C} to PrP^{Sc}.

The normal globular domain of the human PrP^{C} structure contains three α-helices comprising the residues 144–154, 173–194, and 200–228, and a short anti-parallel β-sheet comprising the residues 128–131 and 161–164 [24]. The crystal structures of the human prion protein WT/M129 (1I4M) [24], 4KML [25], and human prion protein variants WT/V129 (3HAK & 3HAF), D178N/M129 (3HEQ), and D178N/V129 (3HJX) [26] have been determined at high resolution and have been shown to occur as swapped (1I4M and 3HAF) or un-swapped (3HEQ, 3HJX) dimers, non-swapped monomers (3HAK) and an ordered N terminus β sheet containing structure stabilized by a nano-molecule (4KML).

The binding modes of known anti-prion molecules are either not known, or have been determined with only the non-swapped structures of PrP^{C}. The pathogenic conversion of PrP^{C} protein into PrP^{Sc} during disease progression involves a process of conformational change that includes domain-swapping. This domain-swapping process could be a crucial step in facilitating the dimerization and subsequent oligomerization of the protein [26]. Small pharmacological compounds that can interfere with this structural transition and oligomerization of the PrP^{C} may potentially inhibit the PrP^{Sc} formation [24]. It is possible that the known anti-prion compounds may exert their inhibitory effects by directly interacting with PrP^{C} or PrP^{Sc}, or by reducing the levels of PrP^{C} through the modulation of various cellular processes [27]. The virtual screening approach for identifying the small compounds targeting the region of the PrP^{C} that interact with the compound GN8 has successfully demonstrated reduction in the amount of PrP^{Sc} in the cells infected with the Rocky Mountain Laboratory scrapie prion strain [11,28].

In our study, we performed *in silico* virtual screening supported by molecular docking against the individual monomers of swapped and non-swapped human PrP^{C} structures to identify eleven compounds from the manually constructed in-house library of phytochemicals with CNS and other publicly available databases with phytochemicals. We also determined their potential binding modes and interactions, which revealed eleven potential novel anti-prion compounds.

2. Material and methods

2.1. Construction of phytochemicals database

For the construction of the in-house library, the plants, which are traditionally used to treat different neurodegenerative diseases, were listed by searching the dendrimer-based drug delivery system [29] on PubMed Central focusing on plants known to have CNS stimulant activity. The bioactive constituents of these plants (phytochemicals) and their derivatives were searched for in the literature and structure databases including Pubmed (described in Supplementary Materials S3), PubChem, Dr. Duke Phytochemical and Ethnobotanical databases, and Traditional Chinese Medicine Database System. The 3D structures of these phytochemicals/bioactives were downloaded from PubChem [30], eMolecules (www.emolecules.com), and ChemSpider [31]. For the structures that were not available, we created them using ACD/Labs 2016 Freeware, v14.00, [32]. In total, we constructed an in-house library of 207 structures of phytochemicals known to act on the CNS.

The final phytochemical compounds library used for docking consisted of a total of 2550 molecules, which included the 207 compounds in our in-house library and additional compounds obtained from various databases, such as AfroDB [33] containing 954 potent natural products from African medicinal plants, $NuBBE_{DB}$ [34] containing 643 bioactives from Atlantic forest, Brazil and IBScreenBioactives (http://www.ibscreen.com) containing 746 biologically active compounds, were downloaded from ZINC databases [35]. Energy minimization was done for all molecules using universal force fields (UFF) from OpenBabel [36,37], before docking to protein structures.

2.2. Target protein and binding pocket preparation

The high-resolution crystal structures of human prion protein PrP^{C} with PDB (Protein Data Bank) accession code 3HAK, 3HAF, 3HEQ, 1I4M, 4KML, and 3HJX were downloaded from the PDB. The water molecules were deleted from all of the six structures, missing amino acids in the 3HEQ and 3HJX were added and the nanomolecule from the 4KML was removed using Accelrys's Discovery Studio Visualiser v16.1.0.153,350 (DassaultSystèmes BIOVIA, BIOVIA Workbook, Release 2017). Energy minimization of the added residues for 3HEQ and 3HJX was done using chimera-1.13.1 [38]. The co-ordinates of the nanomolecule that co-crystallized with PrP^{C} in 4KML were removed, and only the PrP^{C} coordinates were used for docking. The PDB IDs of the structures in the text have been mentioned without the preceding digits and the helices and sheets are mentioned as α and β respectively.

2.3. In silico virtual screening

We performed docking using AutoDock Vina within the open-source software PyRx –Python Prescription 0.8 [39]. The Lamarckian Genetic Search Algorithm with default parameters was used in the automated docking simulation. The search region cubic space encompassed the entire protein and the grid box dimension for respective protein structures (Supplementary Materials S2, Table 1): only monomers (swapped or non-swapped) were included in the docking. The compounds of the in-house database along with compounds shown to have anti-prionic activity, namely GJP49, GN8, and LD7 were also docked against the human PrP^{C} protein as controls.

2.4. Pharmacokinetics and binding mode

The drug-likeness was evaluated, based on 'rule of 5' (Ro5), developed by Lipinski et al. [40] predicted with the online tool PreADMET (http://preadmet.bmdrc.org) for the top 31 compounds based on docking scores. The pharmacokinetic properties of potential anti-prion compounds in the human body, including their absorption, distribution, metabolism, blood-brain barrier penetration, excretion and Toxicity (ADMET) were predicted using AdmetSAR (http://lmmd.ecust.edu.cn/admetsar1). Compounds with binding energies comparable to or higher than the known anti-prion compounds and satisfying the ADMET criteria were selected for analysis

of the binding modes, analysis of interactions, site of fit, and distances using Accelrys's Discovery Studio Visualiser v16.1.0.153,350.

3. Results

31 compounds showed a binding energy that was either comparable to or higher than that of the known anti-prion compounds. The compounds selected for further evaluation in this study are only those that comply with the Lipinski's rule, having no more than one violation of the "rule of 5″ criteria (Supplementary Materials S1, Table 2). Eleven new plant derivatives that can serve as potential inhibitors of PrP^C aggregation are listed in Table 1. All of the compounds are predicted to be absorbed in the intestine and cross the blood-brain barrier, are non-toxic, and non-carcinogenic. They did not inhibit renal organic anion transporters and showed low CYP 450 inhibitory promiscuity. Only RAU25 and BIO115 amongst the new compounds were inhibitors of CYP450 2C9, as was GJP49 from the known anti-prions (Supplementary Materials S1, Tables 1–2).

3.1. Binding energies

Compounds binding to the prion protein through pi-alkyl/alkyl/pi−sigma interactions bind more strongly compared to those that bind through hydrogen bonding. The known anti-prion compounds bound to the swapped structures (mean = −7.31 kcal/mol) more strongly than to the non-swapped structures (mean = −6.59 kcal/mol). The newly identified compounds also bound stronger to the swapped (mean = −9.125 kcal/mol) than to the non-swapped structures (mean = −7.728 kcal/mol) (Supplementary Materials S1, Table 3). The strongest BE (Binding Energies) was that of the compound EA150 to HAF (−10.8 kcal/mol).

3.2. Binding regions

The binding sites for both known and potential anti-prion compounds are illustrated in Fig. 1B for the three types of structures available. All of these compounds bound to the α1-α2 or the α2-α3 loops or to both (Fig. 1A), with a few interactions with residues of the C-termini of α1 and α2. Subunits of swapped dimers had a very small region of binding and very few ionic interactions while binding to non-swapped PrP^C also extended towards the N-terminus of α3 and C-terminus of α2 including the α2-α3 hinge loop residues. Binding to the structure with ordered β sheet N-terminus residues uniquely showed binding throughout α2 and the C-terminus of α3.

3.3. Binding sites: swapped structures

The swapped dimers I4M and HAF structurally aligned with root mean square deviation (r.m.s.d) of 0.294 Å. The known anti-prion compounds interacted with the same regions of the prion protein structures as the new compounds, with the exception of LD7, which

Table 1
List of newly identified plant derivatives, their sources, chemical names, modes of binding and binding energies with the swapped and non-swapped crystal structures. BE-Binding energy, R-alkyl, HB−hydrogen bond.

Comp.	Plant	Chemical name	BE Kcal/mol	Interactions	Regions
3HAF (WT/V129) (Swapped)					
ILE2	*Ilex paraguariensis*	β-amyrin	−8.6	Pro 158 (R), Ile 184(R),Tyr157 (π-R)	α1- α2, α2, α1- α 2
CEN39	*Centella asiatica*	campesterol	−8.3	Tyr149 (π-σ),Tyr145 (π −R), Tyr149 (π −R), Tyr157 (π −R)	N-ter, α 1- α 2
PTY55	*Ptychopetalum olacoides*	β -sitostenone	−8.4	Pro158 (π −R), Tyr157 (π −R), Phe141(π −R),Tyr149 (π −R)	α1-α 2, N-ter, α1
EA150	*African medicinal plant*	(9β,13α) 13,28Epoxyoleanane-3,22-dione	−10.8	Pro137(π −R),Tyr157 (π −R), Tyr150 (π −R), Tyr149 (π −R)	N-ter, α 1-α 2, α 1
I4M (WT/M129) (Swapped)					
PTY55	*Ptychopetalum olacoides*	Stimast-4en-3-one	−8.7	Pro158(R), Tyr157 (π −R), Phe141(π −R)	α 1-α 2, N-ter
CEN39	*Centella asiatica*	Campesterol	−8.4	Phe141(π −R), Pro158(R),Tyr157 (π -σ)	N-ter, α 1-α 2
HAK (WT/V129) (Non-swapped)					
CEN36	*Centella asiatica*	Asiatic Acid	−7.4	His187(Pi-Alkyl), Tyr162 (HB), Thr183(HB)	α 2, β 2
RAU31	*Rauvolfia serpentina*	Rescinnamine	−7.4	Lys194(H-bond), Thr183 (C−H), Tyr162 (HB), Gln160 (C−H), His155(C−H)	α 2, β 2, α 1- α 2
BNP 8864	*Sophora velutina*	Olean-12-en-3-ol	−8.6	His187(Alkyl), His187(Alkyl) Pro158(Alkyl)	α1- α2, α 2
BNP 2069	*Glyptopetalum sclerocarpum*	22-Hydroxytingenone	−8.2	His187 (π −R), Tyr162 (π −R), His155(HB),Arg136(HB)	α 2, β 2, α 1-α 2, N-ter
HEQ (D178N/M129) (Non-swapped)					
RAU25	*Rauvolfia serpentina*	Ajmalicine	−7.8	Thr191(HB), Lys194(HB), Pro158(π -σ)	α 2, α 1-α 2
HJX (D178N/V129 (Non-swapped)					
EPH18	*Ephedra sinica*	Ellagic acid	−7.3	Pro158(π −R), His155(HB), Tyr157(HB), Thr191(HB)	α 1- α 2, α 2
Bio115	*Handroanthus impetiginosus*	atovaquone	−7.4	His155(HB), Tyr157(HB), Asn159(HB)	α 1- α 2
KML (WT-M129 in complex with nanobody Nb484), with Nb484 deleted (Non-swapped)					
RAU31	*Rauvolfia serpentina*	Rescinnamine	−7.1	Tyr163(HB),Asp167(HB),Pro165(π −R), Ala224(HB),Glu221(HB)	β2, α1-α2, C-ter
Bio115	*Handroanthus impetiginosus*	atovaquone	−6.6	Glu207(HB), Thr188 (π -σ), Val203(π −R)	α3, α 2

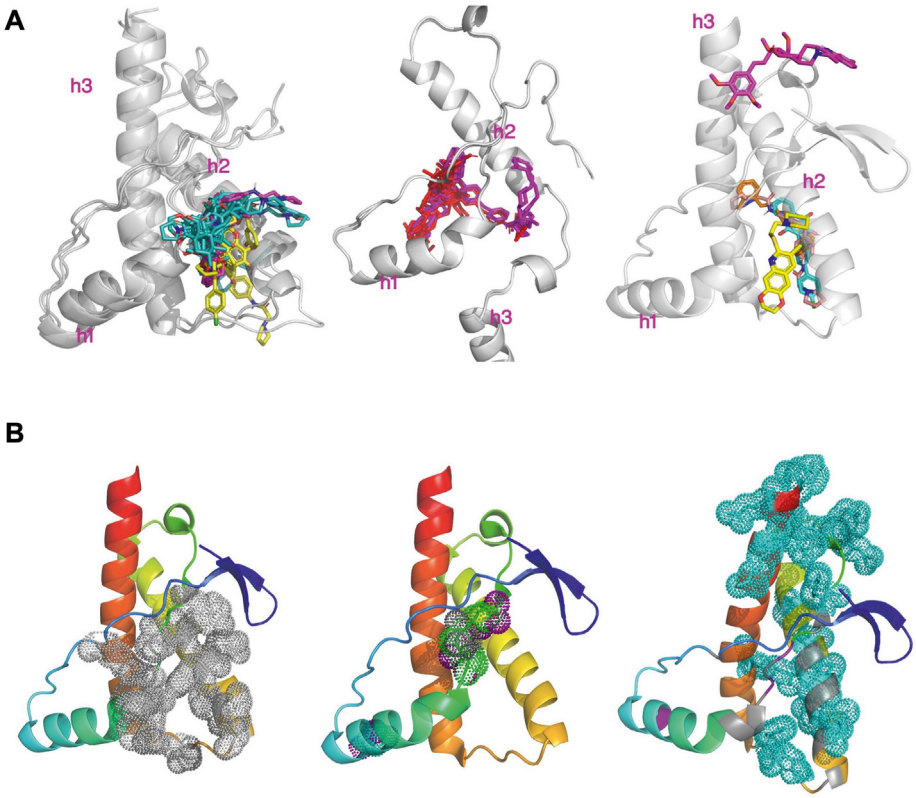

Fig. 1. A: Binding regions of known and new compounds to the non-swapped (left), swapped (center), and non-swapped with ordered N-terminus structures (right). Compounds binding to different structures in the superimposed figures are shown in different colors. B: Regions of prion protein showing regions of interaction. Swapped structures show binding with residues of α2-α 3 regions (left), residues of α 2 and α 3 facing each other as well as residues of α 1 (center) form interactions in the swapped structures, residues throughout α 2, α 2-α 3 switch regions, as well as those of α 3 C-terminus (right), interact with compounds in the ordered N-terminus non-swapped structure. All regions are shown on the ordered N- terminus colored N- to C-terminus (blue to red) structure for comparison.

formed all interactions with α2 (Table 1, Fig. 1A). The number of ionic interactions between swapped monomers and new compounds were very few compared to those of the known compounds, which interacted extensively with all helices and loops. In all cases, the site of binding of these compounds was through hydrophobic residues on α2 which formed the interface of association with α3 of another monomer to form the dimer. Steric clashes of the bound compounds became apparent with α3 when the dimer is created from the compoundbound monomers (Fig. 2A). Monomers of both swapped structures I4M and HAF bound CEN39 and PTY55 in the same regions. However, the known anti-prion compounds LD7 and GJP49 bound with similar binding energies to different sites on I4M and HAF: to a crevice formed by the switch loop and the C-termini of α1 and α2 in I4M versus a surface binding between α1 and α2 in HAF (Fig. 3).

3.4. Binding sites: non-swapped structures

Binding to non-swapped monomers mostly occured to residues of the C-termini of α1 and α2, with some interactions with the α2-α3 switch region (Fig. 1A and B). HAK presented a "tighter" structure as residues 190–194 continues as α2 helix, whereas in other non-swapped structures, they formed a loop. HJX, which presented a more disordered and open α2-α3 loop allowed molecules to extend into the space created by a loosening of this loop. However, only the known anti-prions GJP49 and GN8 were able to occupy this space. Rau31 bound to different sites on HAK and KML which superimposed with r.m.s.d 0.655 Å. The site of binding of RAU31 in KML, involved residues of α3 C-terminus and α2 N-terminus (Figs. 1A and 4B). However, no residue from the N-terminus β sheets was seen to interact with the compound. Bio115 bound to KML as well as HJX (r.m.s.d 1.367 Å) at different sites: to the hinge loop region towards the flip side of α1 in KML whereas in HJX, it bound to the front of the hinge loop facing α1, along with all other compounds. As with other non-swapped structures compared with HJX, the hinge loop region was more organized in KML and tighter, with Thr190 to Lys194 a part of α2 in the latter.

The Binding of compounds in all structures resulted in steric clashes either with the partner monomer or with a crystallographic symmetry-related molecule (Fig. 2B). BIO115 in HJX sterically clashed with another BIO115 as well as its α2-α3 loop on its partner monomer (Fig. 2B(c)). Ligands bound to HAK sterically clashed with residues of three different symmetry-related monomers (Fig. 2B (a)). Steric clashes in HEQ occured only between known anti-prions in the symmetry-related dimers (Fig. 2B (d)). RAU31 in KML sterically clashed with residues from a symmetry-related molecule (Fig. 2B(c)).

3.5. β sheet regions

The residues 188–195 were involved in hydrogen bonding with the same region of the other monomer to form a β sheet in both swapped structures. The known anti-prions LD7 and GJP49 sterically clashed with the Lys194 side chain of the partner monomer in this region in swapped structures. No interactions occured in either type of structures with residues of the β-strand formed by residues

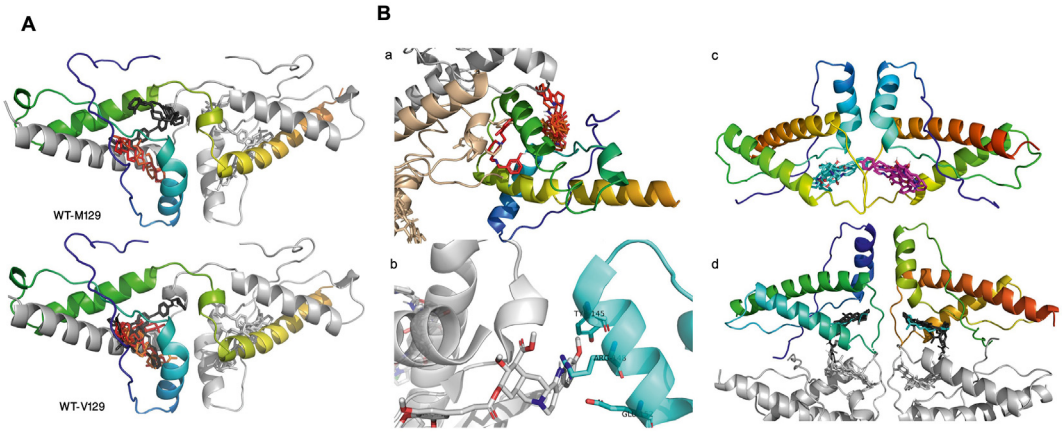

Fig. 2. A: Swapped structure dimers (I4M top and HAF bottom) showed steric clashes of bound molecules bound between α1 and α2 of one monomer (blue to red) with the swapped α3 of the partner monomer (grey). Clashes are also seen with the residues of the switch region of the partner molecule. B: Steric clashes of bound compounds with partner monomers of the dimer and molecules related through crystallographic symmetry in the non-swapped structures. a. HAF showed steric clashes of compounds bound to one monomer (blue to red) with molecules related through crystallographic symmetry (grey and beige) b. Steric clash of RAU31 bound to the C-terminus of KML (grey) with residues of another molecule related through crystallographic symmetry (cyan) c. Steric clashes of bound compounds with each other in the dimer formed in HJX d. Two dimers of compoundbound HEQ showed steric clashes with subunits of another dimer (grey) as well as compounds bound to them, but not with each other (blue to red).

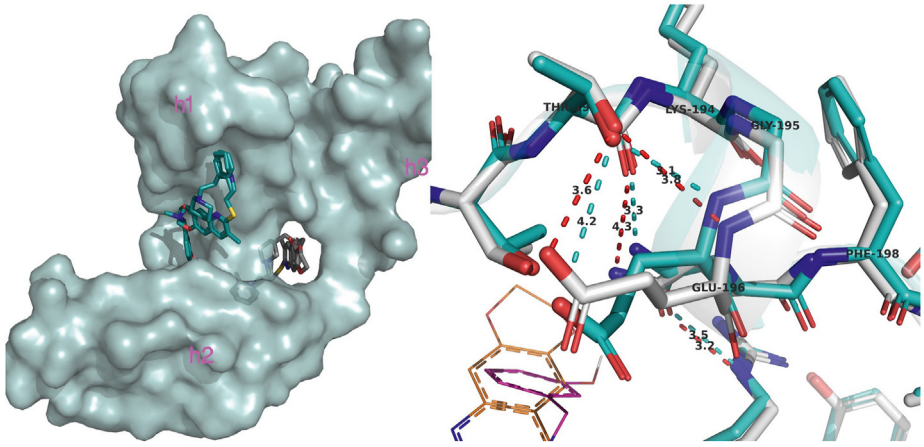

Fig. 3. Differences in binding sites of LD7 and GJP49 to the swapped structures. Bound to HAF on the surface (cyan) while to I4M in the crevice (grey) (Left) when the only difference in the binding regions of either structure was a slight shift in side chain conformations of Glu196 and Asn197 (right) between I4M (grey) and HAF (cyan) so that ionic interactions with surrounding residues changed (red I4M, cyan HAF).

128−131. All new compounds bound to the non-swapped structures interacted with one or the other of Tyr162, Tyr 163, Lys194, Thr188 , and Thr191, which were constituents of β strands in either swapped or non-swapped structures.

4. Discussion

Compounds listed in Table 1 as potential anti-prion compounds bind with comparable or higher binding energies as those of the known anti-prion compounds. The binding sites of the newly found compounds are also the same as the known anti-prion compounds LD7, GJP49, and GN8, with minor differences in residue-specific interactions. None of the new compounds have an extended structure as GN8 or LD7, which can form interactions with more residues and hence, can block more surface area of the protein to prevent association. The new compounds show high binding energy and might not be able to dissociate easily from the protein once they are bound, acting as potential inhibitors by steric hindrance of other prion protein molecules as depicted in Fig. 2A and B. However, high binding energies through docking do not always correlate with binding to PrP^{C} *in vivo* [28], and the sites to which binding occurs on the protein also play an important role in determining the conversion to PrP^{Sc}.

Binding of all known and potential anti-prion compounds in the same region of swapped structures: I4M and HAF is expected, as they are very similar except for the Met and Val respectively at position 129. The binding of LD7 and GJP49 to the two structures at different sites (Fig. 3) highlights the effect of subtle changes in side chain conformations irrespective of the binding energies which are around −7 kcal/mol (Supplementary Materials S1, Table 3). The side-chain conformations of Asn 197 and Glu196 are different in the two structures (Fig. 3), such that the Glu196 side-chain in HAF extends into the cleft that is formed by residues of the switch region. Similarly, the binding of CEN39 to both I4M and HAF is in the same site, but the molecule is flipped to bring the OH group to the opposite end. Although there are slight differences in the side-chain conformations of nearby residues 140−146 in the two structures, these are unlikely to affect CEN39 binding, and both orientations might be possible in a swapped structure. This is reflected in the similar binding energies of CEN39 to both structures (Table 1).

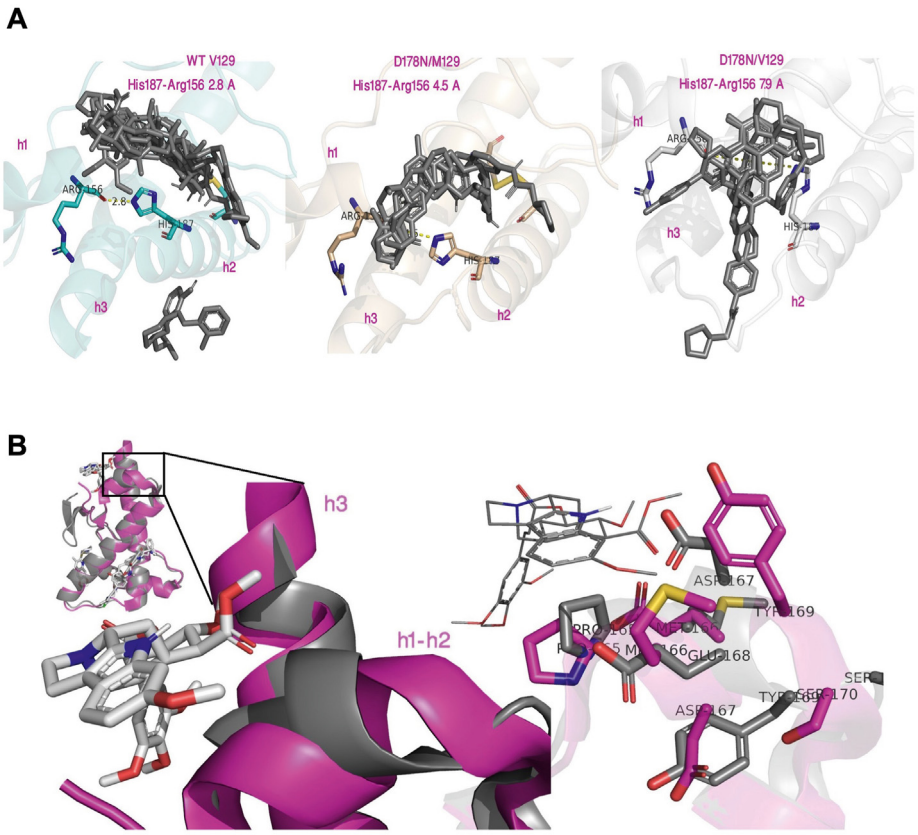

Fig. 4. A: Distances between Arg156 of helix 1 and His 187 of helix 2 in the swapped structures that might determine access to binding of compounds. As h1 moved away, binding shifted towards the h2 −h3 loop Left:HAK, Center: HEQ, Right: HJX Fig. 4B: Differences in binding of RAU31 to HAK (pink) and KML (grey) showed differences in the R164-S170 short helix region (left). Residues in this region are displaced in the two structures (right) and may be responsible for allowing RAU31 (shown in lines) to bind in KML while restricting it in HAK.

The new compounds identified are highly hydrophobic and bind mainly through hydrophobic alkyl and pi−alkyl interactions to residues of α1 (Table 1). It has been proposed that when α1 is caused to either unravel or be pushed away from the α2- α3 subdomain, misfolding is accelerated [41]. Tight binding of compounds to residues of α1 can help stabilize it and prevent its movement. Inhibition of PrP^{C} to PrP^{Sc} conversion by potential anti-prion compounds differs with cell types and correlates with interactions with Asn159 and Glu196 [28]. The ionic interactions between the new compounds and both the swapped structures are very few and encompass Glu146, Pro158, Asn159, and Gln160, while their hydrophobic regions extend along the protein surface. Dimerization of PrP^{C} has been found to be the rate-limiting step during oligomerization and misfolding [41]. As these compounds occupy the region that is filled in by the swapped α3 of another monomer to form a dimer, the prevention of association of α3 of one monomer with α1 of the other can contribute to the inhibitory activity of these compounds towards PrP^{C} to PrP^{Sc} conversion.

There is a shift in the binding of molecules from mainly the hinge loop in HJX towards mostly surface binding to HAK between α1 and α2. The non-swapped structures differ from each other in the rotation of α2 away from the N-terminus of α3. Accompanying the unraveling of the C-termini residues of α2, comprising Thr191 − Lys194, which form an additional helix fold in HAK, are somewhat ordered into a helix in HEQ, and completely disordered in HJX. The energy-minimized structure of this loop in HJX shows Lys194 side chain extended towards the solvent while Asn197 extends towards the protein interior. In the other two structures, Lys 194 turns inwards while Asn 197 extends into the solvent away from the protein surface. LD7 binds to the surface opposite to where the rest of the compounds bind in HAK, which also shows a strong (2.8 A) interaction between the imidazole ring of His187 with the main chain carbonyl oxygen of Arg156. HAK and HJX show larger distances between these residues as shown in Fig. 4A. It is likely that the access to residues in the loop region is reduced due to residues interacting with each other as in HAK.

The conformation of the side chain of Met 166 is flipped in KML compared to HAK so that it is turned towards the C-terminus of the protein. However, in HAK, the Met 166 side chain is turned towards the exterior of the protein and exposed to solvent (Fig. 4B). Similarly, the side chain of Tyr 169 in KML turns towards the interior of the protein, while in HAK it faces the solvent. Although the short helix in this region ranges from Pro165 to Tyr169, the side chains of the residues comprising this region are arranged in different conformations which probably cause the difference in binding of RAU 31 to different regions of these two structures. Residues Tyr162 to Asn171 in KML constitute a loop-β-helix-loop secondary structure domain that interacts closely with the N-terminus β sheet as well as the stabilizing nano-molecule co-crystallized with PrP^{C}. The R164-S170 loop has been suggested to allow transmission of conformational information to influence intermolecular β sheet formation [42]. RAU31 interacts with the small β sheet in both HAK as well as KML and could help disrupt the intermolecular β sheet structures comprising Tyr162, Tyr163, Met/Val129, and Ile 130 seen in the D178N mutants [42]. RAU31 also forms ionic interactions with residues Arg 220, Glu221, and Ala224 of C-terminus α3 in KML. The known anti-malarial drug quinacrine, which has also been shown to be an inhibitor of PrP^{Sc} formation has been shown to bind to

Tyr225, Tyr 226, and Gln 227 of α3 in PrP [43]. Anchorless PrP^C truncated at the C terminus is more prone to PrP^{Sc} formation at low pH [44], presumably due to a decrease in intra-molecular interactions in the C-terminus residues so that they are available for inter-molecular interactions. Following this theory, RAU31 binding to residues of the C-terminus can also decrease the availability of ionic interactions for another PrP monomer, reducing the chances of dimerization. RAU31 hence might be able to act by stabilizing the N- and C- termini, interacting with Asn159, residues of the switch region, and the residues of the intermolecular β sheet, to inhibit PrP^C to PrP^{Sc} conversion.

Based upon *ex vivo* and *in vivo* treatment experiments [45], anti-prion compounds have been proposed to act through specific or non-specific conformational stabilization, reduction of PrP^C through precipitation, and interaction with molecules other than PrP^C [42]. Inhibition of PrP^C to PrP^{Sc} conversion by potential anti-prion compounds differs with cell types and correlates with interactions with Asn159 and Glu196 [28]. Compounds binding to both swapped and non-swapped structures show ionic interactions with Asn159, none interact with Glu196. But many of the newly found compounds strongly interact with Pro158 and Asn197. It can be assumed that the binding of compounds to regions of PrP^C determines inhibition rather than binding to specific amino acids and that binding to residues 158 and 197 will be as effective for inhibition as binding to residues 159 and 196. Moreover, binding to Asn197 is possible only in the non-swapped forms where it is fully exposed. Asn197 is a site of glycosylation of PrP^C [46], and its blocking by an inhibitor can influence both the movement of the hinge region to prevent α3 from swapping as well as by mimicking an *in vivo* glycan as seen in PEGylated (Polyethylene glycol) PrP at 181 and 197 that inhibit PrP^{Sc} formation [47].

A number of studies have shown changes in the conformation of PrP^C resulting from lowering of pH and/or chemical denaturants, and these altered conformation intermediates display one or the other characteristics of PrP^{Sc} [48]. A lowering of pH causes marked chemical shifts in the C- termini of α1 and α2; specifically, Asn186, His187, Thr188, Thr192, Lys194, and Glu196 of α2 and His155, Arg156, and Asn159 of α1 as a result of protonation of His187 and His155 [48]. The protonation of His187 favors PrP^{Sc}-like conformation while de-protonation favors native PrP^C [48]. The known anti-prion compounds LD7, GJP49, and GN8 bind to one or the other of these residues. All new compounds that bind to the non-swapped forms interact either with His155 or His187. Involvement of these histidines in interactions with the compounds might discourage their protonation and hence also the development into an altered conformation intermediate. A low pH treatment of recombinant mouse PrP^C is also accompanied by increased solvent exposure of tyrosine side chains in addition to 25 times higher recognition of PrP^{Sc} by Tyr-Tyr-Arg antibodies compared to PrP^C [49]. The Tyr-Tyr-Arg motif occurs in two regions res.149-151 and res.162-164 in the prion protein. The new compounds stack with one or the other of these tyrosines and also form non-polar interactions with Pro 158 in the swapped monomers. Stacking of rings of the terpenes and sterols can be visualized as tightening hydrophobic interactions and preventing the alteration in the side chain conformations of tyrosines, and by extension of the PrP^{Sc} forming intermediates. Flanking proline residues in prion proteins have also been proposed to have a containment role and confine the β sheet within a specific length [50]. Hydrophobic interactions of compounds with prolines will reinforce its position and hence its role in prevention of lengthening of the β sheet.

All potential new bioactive anti-prion compounds are either tetra- or pentacyclic terpenoids, sterols, or naphthoquinones. Most of these have been shown to be utilized for various medicinal purposes in humans. All of them are able to cross the BBB, bind very strongly to PrP^C, and can prove to be potent anti-prion compounds. Different compounds bind to different forms, the swapped dimer being the least amenable to binding. The presence of the N-terminus β sheet structure might offer more binding sites for stabilization of the soluble monomeric form and prevention of dimerization.

Rau25 or Ajmalicine is an α1 adrenergic receptor antagonist used as an anti-hypertensive drug [51]. It is a heteropentacyclic monoterpenoid indole alkaloid and methyl ester found in the root or bark of several plant species including Rauwolfia spp, *Catharanthus rosea* etc [52]. RAU31 or Rescinnamine, is a heteropentacylic vinca alkaloid also derived from *Rauwolfia serpentina* and other species of Rauwolfia [53] used as an antihypertensive drug and an angiotensin converting enzyme inhibitor.

CEN36 (Asiatic acid) and CEN39 (campesterol) are triterpene and sterol derivatives respectively from *Centella asiatica*. *C. asiatica* contains a variety of saponins, of which asiaticoside, an asiatic acid derivative, has been suggested to exert a therapeutic effect in Alzheimer's disease [54]. Asiatic acid has also been found to be neuroprotective in a mouse model of focal cerebral ischemia [55]. *C. asiatica* synthesizes saponins (triterpenes) including asiatic acid and sterols including campesterol from mevalonic acid via the isoprenoid pathway [56]. Campesterol has been demonstrated to be able to cross the BBB in mice [57]. There is no flux of lipoprotein-bound cholesterol across the BBB, but the presence of an alkyl group on the 24-position of cholesterol side chain (campesterol) results in a markedly increased ability to cross the intact BBB [58].

BNP2069(22 hydroxytingenone or tingenin B), a pentacyclic quinine methide triterpenoid compound has been found to possess antibacterial, antiparasitic, and anticancer activities [59]. BNP8864 and ILE2 are different representations of olean-12en-3-ol or β-amyrin, a very commonly occurring pentacyclic triterpenoid that is oleanane substituted at the β position by a hydroxyl group, with a double bond between C12 and C13 and is found in many higher plant species [60]. β amyrin has been found to ameliorate the cognitive impairment induced by hypocholinergic neurotransmission, as seen in Alzheimer's disease, via the activation of ERK as well as GSK-3 β signaling [61].

PTY55 β-sitostenone (Stigmast-4en-3-one) is a steroid derivative present in many plant species. β-sitosterone and its corresponding alcohol β sitosterol from *Anacardium occidentale* (cashew) have been shown to have hypoglycemic activity demonstrated through an intravenous injection in healthy dogs [62]. EPH18 or ellagic acid is a natural polyphenol heterotetracyclic antioxidant derived from gallic acid, that occurs in numerous fruits and vegetables, especially in black raspberries and pomegranate juice. Ellagic acid has been found to exhibit antioxidant and anticarcinogenic properties, including inhibition of tumor formation and growth both *in vitro* and *in vivo* [63,64]. Ellagic acid possesses potent neuroprotective effects through its free radical scavenging properties, iron chelation, activation of different cell signaling pathways, and mitigation of mitochondrial dysfunction [65]. Bio115 or atovaquone is a synthetic derivative of lapachol from *Tabebuia* species (Bignoniaceae). Atovaquone is an anti-malarial drug that inhibits the electron transport chain by binding to the quinol oxidation site of cytochrome *bc*1 complex [66]. EA150 is a compound from the natural product library of African medicinal plants [67]. There is not much information about this compound and its utility in medicine, except for its listing in the ZINC database [68]. It is a derivative of the pentacyclic triterpenoid oleanane [69].

One of the limitations of this study is that we could not assess whether these compounds bind to the disordered N-terminal domain of PrP^C as these structures are not available in the PDB. In addition, helix swapping has potentially important implications for prion diseases, however, the physiological relevance of this 3D

domain-swapped dimer protein structure is poorly studied or at present unknown. Moreover, ADMET prediction does not assure real pharmacokinetics properties but only provides guidance in *silico* drug screening. Molecular docking methods have many advantages in drug discovery tasks. However, the results should be supported by experimental data [70]. Thus, identified compounds need to be further evaluated *in vitro* and *in vivo* for their effectiveness.

5. Conclusion

The newly identified compounds are derivatives of terpenes, sterols, and quinones, and they bind to the same regions of PrP^C as the known anti-prion compounds. The conformation of PrP^C to which these compounds bind differs and their mechanism of action may involve multiple effects ranging from steric hindrance of association of monomers, blocking of the swapping of α3 towards α2, stabilizing the switch region between α2 and α3, preventing protonation of histidines, and reducing exposure of tyrosines to the solvent. As some of these compounds are used for medicinal purposes for various conditions, they form an attractive group of compounds to study further for the prevention of PrP^C to PrP^{Sc} conversion, either in isolation or in combination with each other. Interestingly, this approach and phytochemical library used in this present study may be relevant for performing *in silico* screening against several other neurodegenerative conditions. However, the validation of these novel potential anti-prion compounds further requires *in vitro* surface plasmon resonance analysis, NMR, *in vitro* cell line cultures, and *in vivo* mouse models are indispensable.

Authors' contributions

SN built the in-house library of phytochemicals, performed autodocking, contributed to manuscript writing and revisions. JK and SR contributed to creation of database. ASP planned and supervised the docking, carried out structural analysis and contributed to manuscript writing. All authors have read and approved the final manuscript.

Funding

This research did not receive any specific grant from funding agencies in the public, commercial, or not- or-profit sectors.

Declaration of competing interest

None.

Acknowledgements

Not applicable.

Abbreviation

ADMET	absorption, distribution, metabolism, elimination, toxicity
BBB	Blood–brain barrier
BE	Binding Energies
BIO115	atovaquone
BNP2069	22 - Hydroxytingenone
BNP8864	Olean-12-en-3-ol
CEN36	Asiatic acid
CEN39	Campesterol
CNS	Central Nervous System
EA150	(9β 13 α) 13,2 8-Epoxyoleanane-3,22 dione
EPH18	Ellagic acid
ILE2	β-amyrin
PEG	polyethyleneglycol
PrP	Prion Protein
PrP^C	Cellular prion protein
PrP^{res}	Protease-resistant prion protein
PrP^{Sc}	Pathogenic scrapie prion
PTY55	β-sitostenone
r.m.s.d.	root mean square deviation
RAU 31	Rescinnamine
RAU25	Ajmalicine
TSE	Transmissible Spongiform Encephalopathy
UFF	Universal force fields

Appendix A. Supplementary data

Supplementary data to this article can be found online at https://doi.org/10.1016/j.jaim.2023.100750.

References

[1] Prusiner SB. Nobel lecture: prions. Proc Natl Acad Sci USA 1998;95:13363–83. https://doi.org/10.1073/pnas.95.23.13363.
[2] Cunha JEG, Nascimento JCF, Oliveira JRM. CJD without borders. Nat Rev Neurol 2021;17:723. https://doi.org/10.1038/s41582-021-00566-w. 723.
[3] Kupfer L, Hinrichs W, Groschup MH. Prion protein misfolding. Curr Mol Med 2009;9:826–35. https://doi.org/10.2174/156652409789105543.
[4] Yamamoto N, Kuwata K. Regulating the conformation of prion protein through ligand binding. J Phys Chem B 2009;113:12853–6. https://doi.org/10.1021/jp905572w.
[5] Aguzzi A, De Cecco E. Shifts and drifts in prion science. Science 2020;370:32–4. https://doi.org/10.1126/science.abb8577.
[6] Diaz-Espinoza R, Morales R, Concha-Marambio L, Moreno-Gonzalez I, Moda F, Soto C. Treatment with a non-toxic, self-replicating anti-prion delays or prevents prion disease in vivo. Mol Psychiatr 2017;1–12. https://doi.org/10.1038/mp.2017.84.
[7] Cashman NR, Caughey B. Prion diseases - close to effective therapy? Nat Rev Drug Discov 2004;3:874–84. https://doi.org/10.1038/nrd1525.
[8] Kocisko DA, Baron GS, Rubenstein R, Chen J, Kuizon S, Caughey B. New inhibitors of scrapie-associated prion protein formation in a library of 2000 drugs and natural products. J Virol 2003;77:10288–94. https://doi.org/10.1128/JVI.77.19.10288.
[9] Zattoni M, Legname G. Tackling prion diseases: a review of the patent landscape. Expert Opin Ther Pat 2021;31:1097–115. https://doi.org/10.1080/13543776.2021.1945033.
[10] Messer A, Butler DC. Optimizing intracellular antibodies (intrabodies/nanobodies) to treat neurodegenerative disorders. Neurobiol Dis 2020;134:104619. https://doi.org/10.1016/j.nbd.2019.104619.
[11] Ishibashi D, Nakagaki T, Ishikawa T, Atarashi R, Watanabe K, Cruz FA, et al. Structure-based drug discovery for prion disease using a novel binding simulation. EBioMedicine 2016;9:238–49. https://doi.org/10.1016/j.ebiom.2016.06.010.
[12] Baldi A. Computational approaches for drug design and discovery: an overview. Sys Rev Pharm 2010;1:99–105. https://doi.org/10.4103/0975-8453.59519.
[13] Singh DB. Success, limitation and future of computer aided drug designing. Transl Med 2014;4. https://doi.org/10.4172/2161-1025.1000e127.
[14] Talele T, Khedkar S, Rigby A. Successful applications of computer aided drug discovery: moving drugs from concept to the clinic. Curr Top Med Chem 2010;10:127–41. https://doi.org/10.2174/156802610790232251.
[15] Pagadala NS, Syed K, Bhat R. In silico strategies on prion pathogenic conversion and inhibition from PrP^C–PrP^{Sc}. Expet Opin Drug Discov 2017;12:241–8. https://doi.org/10.1080/17460441.2017.1287171.
[16] Kuwata K, Nishida N, Matsumoto T, Kamatari YO, Hosokawa-Muto J, Kodama K, et al. Hot spots in prion protein for pathogenic conversion. Proc Natl Acad Sci U S A 2007;104:11921. https://doi.org/10.1073/pnas.0702671104. 6.
[17] Hosokawa-Muto J, Kamatari YO, Nakamura HK, Kuwata K. Variety of antiprion compounds discovered through an in silico screen based on cellular-form prion protein structure: correlation between antiprion activity and binding affinity. Antimicrob Agents Chemother 2009;53:765–71. https://doi.org/10.1128/AAC.01112-08.
[18] Yan C, Zhou Z. Ellagic acid and pentagalloylglucose are potential inhibitors of prion protein fibrillization. Int J Biol Macromol 2021;172:371–80. https://doi.org/10.1016/j.ijbiomac.2021.01.045.
[19] Sirohi PR, Kumari A, Admane N, Somvanshi P, Grover A. The polyphenolic phytoalexin polydatin inhibits amyloid aggregation of recombinant human prion protein. RSC Adv 2021;11:25901–11. https://doi.org/10.1039/D1RA01891D.

[20] Imberdis T, Heeres JT, Yueh H, Fang C, Zhen J, Rich CB, et al. Identification of anti-prion compounds using a novel cellular assay. J Biol Chem 2016;291: 26164–76. https://doi.org/10.1074/jbc.M116.745612.
[21] Eiden M, Leidel F, Strohmeier B, Fast C, Groschup MH. A medicinal herb Scutellaria lateriflora inhibits PrP replication in vitro and delays the onset of prion disease in mice. Front Psychiatr 2012;3:1–8. https://doi.org/10.3389/fpsyt.2012.00009.
[22] Rubia K, Alegria A, Brinson H. Imaging the ADHD brain : medication effects and clinical translation. Expert Rev Neurother 2014;14:519–38. https://doi.org/10.1016/j.pharmthera.2009.04.002.Ethnobotany.
[23] Mendes FR, Negri G, Duarte-Almeida JM, Tabach R, Carlini EA. The action of plants and their constituents on the central nervous system. Plant Bioactives and Drug Discovery: Principles, Practice, and Perspectives 2012:161–204. https://doi.org/10.1002/9781118260005.ch5.
[24] Knaus KJ, Morillas M, Swietnicki W, Malone M, Surewicz WK, Yee VC. Crystal structure of the human prion protein reveals a mechanism for oligomerization. Nat Struct Biol 2001;8:770–4. https://doi.org/10.1038/nsb0901-770.
[25] Abskharon RNN, Giachin G, Wohlkonig A, Soror SH, Pardon E, Legname G, et al. Probing the N-terminal β-sheet conversion in the crystal structure of the human prion protein bound to a nanobody. J Am Chem Soc 2014;136:937–44. https://doi.org/10.1021/ja407527p.
[26] Lee S, Antony L, Hartmann R, Knaus KJ, Surewicz K, Surewicz WK, et al. Conformational diversity in prion protein variants influences intermolecular ??-sheet formation. EMBO J 2010;29:251–62. https://doi.org/10.1038/emboj.2009.333.
[27] Ferreira NC. Anti - prion activity of a panel of aromatic chemical compounds : in vitro and in silico approaches, vols. 2–25; 2016. https://doi.org/10.1371/journal.pone.0084531.
[28] Hyeon JW, Choi J, Kim SY, Govindaraj RG, Hwang KJ, Lee YS, et al. Discovery of novel anti-prion compounds using in silico and in vitro approaches. Sci Rep 2015;5:14944. https://doi.org/10.1038/srep14944.
[29] Wang B, Editor S. Wiley series in drug discovery and development. Dendrimer-based drug delivery systems, vols. 515–6; 2012. https://doi.org/10.1002/9781118275238.scard.
[30] Kim S, Thiessen PA, Bolton EE, Chen J, Fu G, Gindulyte A, et al. PubChem substance and compound databases. Nucleic Acids Res 2016;44:D1202–13. https://doi.org/10.1093/nar/gkv951.
[31] Pence HE, Williams A. Chemspider: an online chemical information resource. J Chem Educ 2010;87:1123–4. https://doi.org/10.1021/ed100697w.
[32] Li Z, Wan H, Shi Y, Ouyang P. Personal experience with four kinds of chemical structure drawing software: review on chemdraw, chemwindow, ISIS/draw, and chemsketch. J Chem Inf Comput Sci 2004;44:1886–90. https://doi.org/10.1021/ci049794h.
[33] Ntie-Kang F, Zofou D, Babiaka SB, Meudom R, Scharfe M, Lifongo LL, et al. AfroDb: a select highly potent and diverse natural product library from african medicinal plants. PLoS One 2013;8:e78085. https://doi.org/10.1371/journal.pone.0078085.
[34] Valli M, Dos Santos RN, Figueira LD, Nakajima CH, Castro-Gamboa I, Andricopulo AD, et al. Development of a natural products database from the biodiversity of Brazil. J Nat Prod 2013;76:439–44. https://doi.org/10.1021/np3006875.
[35] Sterling T, Irwin JJ. ZINC 15 - ligand discovery for everyone. J Chem Inf Model 2015;55:2324–37. https://doi.org/10.1021/acs.jcim.5b00559.
[36] O'Boyle NM, Banck M, James CA, Morley C, Vandermeersch T, Hutchison GR. Open babel: an open chemical toolbox. J Cheminf 2011;3:1–14. https://doi.org/10.1186/1758-2946-3-33.
[37] Dallakyan S. Small-molecule library screening by docking with PyRx, vol. 1263; 2015. https://doi.org/10.1007/978-1-4939-2269-7.
[38] Pettersen EF, Goddard TD, Huang CC, Couch GS, Greenblatt DM, Meng EC, et al. UCSF Chimera - a visualization system for exploratory research and analysis. J Comput Chem 2004;25:1605–12. https://doi.org/10.1002/jcc.20084.
[39] Trott O, Olson A. AutoDock Vina: improving the speed and accuracy of docking with a new scoring function, efficient optimization and multithreading. J Comput Chem 2010;31:455–61. https://doi.org/10.1002/jcc.21334.AutoDock.
[40] Lipinski CA, Lombardo F, Dominy BW, Feeney PJ. Experimental and computational approaches to estimate solubility and permeability in drug discovery and develop ment settings. Adv Drug Deliv Rev 1997;23:3–25. https://doi.org/10.1016/S0169–409X(00)00129-0.
[41] Sabareesan AT, Udgaonkar JB. Pathogenic mutations within the disordered palindromic region of the prion protein induce structure therein and accelerate the formation of misfolded oligomers. J Mol Biol 2016;428:3935–47. https://doi.org/10.1016/j.jmb.2016.08.015.
[42] Lee S, Antony L, Hartmann R, Knaus KJ, Surewicz K, Surewicz WK, et al. Conformational diversity in prion protein variants influences intermolecular β-sheet formation. EMBO J 2010;29:251–62. https://doi.org/10.1038/emboj.2009.333.
[43] Vogtherr M, Grimme S, Elshorst B, Jacobs DM, Fiebig K, Griesinger C, et al. Antimalarial drug quinacrine binds to C-terminal helix of cellular prion protein. J Med Chem 2003;46:3563–4. https://doi.org/10.1021/jm034093h.
[44] Kovač V, Hafner-Bratkovič I, Čurin Šerbec V. Anchorless forms of prion protein – impact of truncation on structure destabilization and prion protein conversion. Biochem Biophys Res Commun 2016;481:1–6. https://doi.org/10.1016/j.bbrc.2016.11.036.
[45] Kamatari YO, Hayano Y, Yamaguchi KI, Hosokawa-Muto J, Kuwata K. Characterizing antiprion compounds based on their binding properties to prion proteins: implications as medical chaperones. Protein Sci 2013;22:22–34. https://doi.org/10.1002/pro.2180.
[46] Aguzzi A, Baumann F, Bremer J. The prion's elusive reason for being. Annu Rev Neurosci 2008;31:439–77. https://doi.org/10.1146/annurev.neuro.31.060407.125620.
[47] Araman C, Thompson RE, Wang S, Hackl S, Payne RJ, Becker CFW. Semisynthetic prion protein (PrP) variants carrying glycan mimics at position 181 and 197 do not form fibrils †Electronic supplementary information (ESI) available. See DOI: 10.1039/c7sc02719b Click here for additional data file. Chem Sci 2017;8:6626–32. https://doi.org/10.1039/c7sc02719b.
[48] Hosszu LLP, Tattum MH, Jones S, Trevitt CR, Wells MA, Waltho JP, et al. The H187R mutation of the human prion protein induces conversion of recombinant prion protein to the PrP(Sc)-like form. Biochemistry 2010;49:8729–38. https://doi.org/10.1021/bi100572j.
[49] Paramithiotis E, Pinard M, Lawton T, LaBoissiere S, Leathers VL, Zou W-Q, et al. A prion protein epitope selective for the pathologically misfolded conformation. Nat Med 2003;9:893–9. https://doi.org/10.1038/nm883.
[50] Shamsir MS, Dalby AR. β-Sheet containment by flanking prolines: molecular dynamic simulations of the inhibition of β-sheet elongation by proline residues in human prion protein. Biophys J 2007;92:2080–9. https://doi.org/10.1529/biophysj.106.092320.
[51] Ajmalicine (CHEBI:2524) https://www.ebi.ac.uk/chebi/searchId.do;?chebiId=CHEBI:2524. Accessed 23 May 2019.
[52] Chopra R, Nayar S, Chopra I. Full text of "glossary of Indian medicinal plants (1956). New Delhi, India: Council of Scientific and Industrial Research; 1956. https://archive.org/stream/in.ernet.dli.2015.507107/2015.507107.Glossary-Of_djvu.txt. [Accessed 23 May 2019].
[53] Fife R, Maclaurin JC, Wright JH. Rescinnamine in treatment of hypertension in hospital clinic and in general practice. Br Med J 1960;2:1848–50. https://doi.org/10.1136/bmj.2.5216.1848.
[54] Mook-Jung I, Shin JE, Yun SH, Huh K, Koh JY, Park HK, et al. Protective effects of asiaticoside derivatives against beta-amyloid neurotoxicity. J Neurosci Res 1999;58:417–25. https://doi.org/10.1002/(SICI)1097-4547(19991101)58:3<417::AIDJNR7>3.0.CO;2-G.
[55] Krishnamurthy RG, Senut M-C, Zemke D, Min J, Frenkel MB, Greenberg EJ, et al. Asiatic acid, a pentacyclic triterpene from Centella asiatica, is neuroprotective in a mouse model of focal cerebral ischemia. J Neurosci Res 2009;87:2541–50. https://doi.org/10.1002/jnr.22071.
[56] Kim OT, Kim SH, Ohyama K, Muranaka T, Choi YE, Lee HY, et al. Upregulation of phytosterol and triterpene biosynthesis in Centella asiatica hairy roots overexpressed ginseng farnesyl diphosphate synthase. Plant Cell Rep 2010;29:403–11. https://doi.org/10.1007/s00299-010-0831-y.
[57] Vanmierlo T, Weingärtner O, Pol SVD, Husche C, Kerksiek A, Friedrichs S, et al. Dietary intake of plant sterols stably increases plant sterol levels in the murine brain. JLR (J Lipid Res) 2012;53:726–35. https://doi.org/10.1194/jlr.M017244.
[58] Saeed AA, Genové G, Li T, Hülshorst F, Betsholtz C, Björkhem I, et al. Increased flux of the plant sterols campesterol and sitosterol across a disrupted blood brain barrier. Steroids 2015;99:183–8. https://doi.org/10.1016/j.steroids.2015.02.005.
[59] Cevatemre B, Botta B, Mori M, Berardozzi S, Ingallina C, Ulukaya E. The plant-derived triterpenoid tingenin B is a potent anticancer agent due to its cytotoxic activity on cancer stem cells of breast cancer in vitro. Chem Biol Interact 2016;260:248–55. https://doi.org/10.1016/j.cbi.2016.10.001.
[60] Hernndez L, Palazon J, Navarro-Oca A. The pentacyclic triterpenes alpha, beta-amyrins: a review of sources and biological activities. In: Rao V, editor. Phytochemicals - a global perspective of their role in nutrition and health. InTech; 2012. p. 491. https://doi.org/10.5772/27253.
[61] Park SJ, Ahn YJ, Oh SR, Lee Y, Kwon G, Woo H, et al. Amyrin attenuates scopolamine-induced cognitive impairment in mice. Biol Pharm Bull 2014;37: 1207–13. https://doi.org/10.1248/bpb.b14-00113.
[62] Alexander-Lindo RL, Morrison EYSA, Nair MG. Hypoglycaemic effect of stigmast-4-en-3-one and its corresponding alcohol from the bark of Anacardium occidentale (cashew). Phytother Res: PT 2004;18:403–7. https://doi.org/10.1002/ptr.1459.
[63] Vanella L, Di Giacomo C, Acquaviva R, Barbagallo I, Cardile V, Kim DH, et al. Apoptotic markers in a prostate cancer cell line: effect of ellagic acid. Oncol Rep 2013;30:2804–10. https://doi.org/10.3892/or.2013.2757.
[64] Eskra JN, Schlicht MJ, Bosland MC. Effects of black raspberries and their ellagic acid and anthocyanin constituents on taxane chemotherapy of castration-resistant prostate cancer cells. Sci Rep 2019;9:4367. https://doi.org/10.1038/s41598-019-39589-1.
[65] Ahmed T, Setzer WN, Nabavi SF, Orhan IE, Braidy N, Nabavi ES-S, et al. Insights into effects of ellagic acid on the nervous system: a mini review. Curr Pharmaceut Des 2016;22:1350–60. https://doi.org/10.2174/1381612822666160125114503.

[66] Fisher N, Abd Majid R, Antoine T, Al-Helal M, Warman AJ, Johnson DJ, et al. Cytochrome b mutation Y268S conferring atovaquone resistance phenotype in malaria parasite results in reduced parasite bc1 catalytic turnover and protein expression. J Biol Chem 2012;287:9731–41. https://doi.org/10.1074/jbc.M111.324319.

[67] Ntie-Kang F, Zofou D, Babiaka SB, Meudom R, Scharfe M, Lifongo LL, et al. AfroDb: a select highly potent and diverse natural product library from african medicinal plants. PLoS One 2013;8:e78085. https://doi.org/10.1371/journal.pone.0078085.

[68] ZINC95486072 | ZINC Is Not Commercial - a database of commercially-available compounds http://zinc.docking.org/substance/95486072. Accessed 11 June 2019.

[69] ((9β,13α)-13,28-Epoxyoleanane-3,22-dione | C30H46O3 | ChemSpider http://www.chemspider.com/Chemical-Structure.68899531.html?rid=84d90b9d-d6f7-4f21-a847-f08f132b209a. Accessed 11 June 2019.

[70] Pinzi L, Rastelli G. Molecular docking: shifting paradigms in drug discovery. Int J Math Stat 2019;20:4331. https://doi.org/10.3390/ijms20184331.